

An experimental study on seepage behavior of sandstone material with different gas pressures

Sheng-Qi Yang¹ · Yan-Hua Huang¹ · Yu-Yong Jiao² · Wei Zeng¹ · Qing-Lei Yu³

Received: 18 June 2014 / Revised: 7 August 2014 / Accepted: 5 January 2015 / Published online: 16 July 2015

© The Chinese Society of Theoretical and Applied Mechanics; Institute of Mechanics, Chinese Academy of Sciences and Springer-Verlag Berlin Heidelberg 2015

Abstract The seepage evolution characteristic of brittle rock materials is very significant for the stability and safety of rock engineering. In this research, a series of conventional triaxial compression and gas seepage tests were carried out on sandstone specimens with a rock mechanics servo-controlled testing system. Based on the experimental results, the relationship between permeability and deformation is firstly analyzed in detail. The results show that the permeability–axial strain curve can be divided into the following five phases: the phase of micro-defects closure, the phase of linear elastic deformation, the phase of nonlinear deformation, the phase of post-peak stress softening and the phase of residual strength. The seepage evolution characteristic is also closely correlated with the volumetric deformation according to the relationship between permeability and volumetric strain. It is found that the gas seepage pressure has a great effect on the permeability evolution, i.e. permeability coefficients increase with increasing gas seepage pressures. Finally, the influence of gas seepage pressures on the failure behavior of brittle sandstone specimens is discussed.

Keywords Rock mechanics · Sandstone · Gas seepage · Volumetric deformation · Permeability

1 Introduction

The mechanism of rock and fluid coupling is very important in many rock mass engineering fields, for instance, underground, dam, rock slope, and nuclear waste storage engineering. Permeability is an important index to reflect the ability of fluid migration in rocks. Permeability characteristics are closely related to the micro-structural damage induced by rock deformation and failure process under loading or unloading. The seepage evolution characteristic of brittle rock materials is very significant for the stability and safety of rock engineering.

The effect of pore pressure, confining pressure and stress level on the seepage behavior of rock material has been widely investigated by using a servo-controlled testing system. The transport properties of low porous rock salt was studied by Schulze et al. [1], who described the conditions for the transition from non-dilatant to dilatant deformation. Their results showed that pore pressure affects the mechanical properties of damaged and dilated rock salt. Four types of rock materials, i.e., mudstone, sandy shale, fine sandstone, and medium sandstone, were tested by Wang and Park [2] under triaxial compression to investigate the relationship between permeability and complete stress–strain process. They found that the permeability is not a constant, but changes with the stress and strain in the rocks. Triaxial compression tests for Luogu basalt with permeability measurement under different confining pressures were performed by Jiang et al. [3]. The effect of confining pressure on permeability evolution curves were presented before peak stress

✉ Sheng-Qi Yang
yangsqi@hotmail.com

¹ State Key Laboratory for Geomechanics and Deep Underground Engineering, School of Mechanics and Civil Engineering, China University of Mining and Technology, Xuzhou 221116, China

² Institute of Rock and Soil Mechanics, Chinese Academy of Sciences, Wuhan 430071, China

³ School of Resource and Civil Engineering, Northeastern University, Shenyang 110819, China

and a micromechanics-based model was proposed in their study. In order to study the relationship between the deformation mechanism and permeability on brittle rock, Zhang et al. [4] carried out a series of triaxial compression tests for limestone, medium sandstone, and fine sandstone. The analysis results of the permeability and stress–strain curves and the relationship between strain corresponding to maximum and minimum permeability and confining pressure showed that the permeability increased rapidly at a critical failure point due to serious microstructural damage. Three kinds of fractured rock, i.e., mudstone, limestone, and sandstone specimens, were tested by Ma et al. [5] to study the seepage properties of fractured rocks under different confining pressures. The study by Wang et al. [6] analyzed the fluid flow and the effects of the confining pressures on the fluid flow and discussed the fluid flow characteristics with complete stress–strain curves. A number of transient pulse tests and steady flow tests were carried out by Tan et al. [7] on Eibenstock granite specimens to investigate the permeability evolution law with the volumetric strain, and established a modified elemental constitutive law on the basis of the Hoek–Brown failure criterion. In addition, some other researchers [8–13] also investigated the permeability evolution laws during the rock damage process under different conditions.

Based on micromechanical analysis and experimental evidence from rock materials, some theoretical and numerical models need to be developed to understand deeply the seepage behavior. By taking into account the variation of permeability, Zhou et al. [14] proposed an anisotropic damage model of brittle rock. A conceptual model and a micro-kinematics mechanism of micro-cracking were constructed by Wang et al. [15]. Compared with the tested data, their model could predict the permeability evolution and better describe the macro-experimental phenomenon before the peak permeability evolution. The study by Pereira and Arson [16] derived a permeability model for unsaturated cracked porous media, while other models such as a revised mathematical model for seepage of deeply buried groundwater [17], a coupled non-linear elastic deformation and non-steady seepage flow model [18], and a promising homogenization based formulation [19] were proposed for different applications. Furthermore, some numerical methods were applied to study the coupling between permeability and damage evolution. A flow-stress-damage (FSD) model was used by Tang et al. [20] to simulate the behavior of fluid flow and damage evolution by F-RFPA^{2D}. The numerical study results suggested that fluid flow strongly depends upon the heterogeneity of the rocks and varies with different rock materials. A three-dimensional numerical manifold method was proposed by Jiang et al. [21] for unconfined seepage analysis. The simulation results showed that the approach could be used to analyze the unconfined seepage behavior.

The research by Ou et al. [22] established a calculation model and analyzed the effect of mining pressure and plastic damage on pore water pressure and seepage vector change rule by FLAC^{3D}.

The previous studies have demonstrated the close relationship between permeability and stress level, and also helped us understand the permeability characteristics and deformation behaviors of rock materials under hydro-mechanical coupling. However, previously, many people focused on the stage before peak strength, while the permeability characteristics at the stage of post-peak strength, especially the stage of residual strength, have been less studied. In other words, only a few experimental works have been conducted to study permeability evolution during the entire deformation and failure process. In this study, based on a rock mechanics servo-controlled testing machine, a series of sandstone triaxial compression tests are conducted for a certain confining pressure and different gas seepage pressures to investigate the evolution law of gas permeability with the axial strain, radial strain, and volumetric strain, the relationship between gas seepage pressure and permeability, as well as the failure characteristics under different gas seepage pressures.

2 Experimental material and loading procedure

2.1 Experimental material

The material used throughout this study was sandstone (collected from the Linyi city, Shandong province of China). Sandstone (Fig. 1) is a fine- to medium-grained, feldspathic rock material with a connected porosity of 5.3 % and a bulk density of 2450 kg/m³. The results of X-ray diffraction (XRD) show that the minerals in the sandstone specimens are mainly feldspar, quartz, and smectite. In this research, the P-wave velocity and S-wave velocity of sandstone are 2873 and 1772 m/s, respectively. Basic parameters of the tested sandstone specimens and conditions are listed in Table 1. All experiments were carried out on cylindrical specimens of 25 mm in diameter and 50 mm in height.

The microstructure surface images of sandstone specimens enlarged 200, 600, and 1000 times by scanning electronic microscope (SEM) are shown in Fig. 1. As shown in Fig. 1, the geometric shape of most of the mineral grains are irregular lumps and most are linked together. However, as we can see, there are some microscopic flaws among the grains, including micro-pores and micro-cracks. In rock materials, these microscopic flaws in isolation may have much less tensile and compression strength than that of the rock continuum. It should be noted that the microscopic flaws become the initial seepage channels, thus fluid can move inside the specimens.

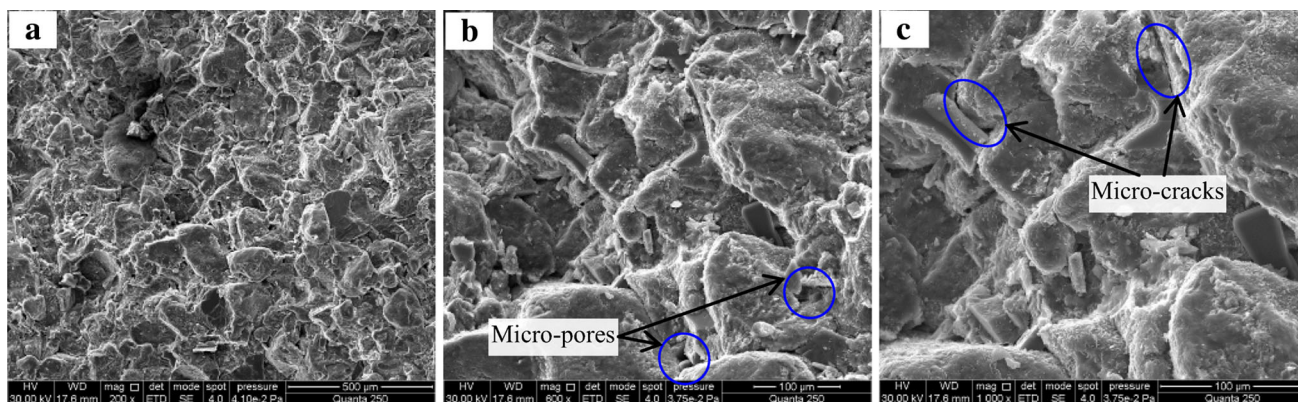


Fig. 1 SEM images of microstructure **a** Enlarged 200 times. **b** Enlarged 600 times. **c** Enlarged 1000 times

Table 1 Basic parameters of sandstone specimens under triaxial compression

Specimen	D (mm)	H (mm)	M (g)	ρ (g/cm ³)	σ_3 (MPa)	P_g (MPa)
C4 [#]	25.1	50.4	60.28	2.417	20	2.0
C5 [#]	25.1	51.3	62.99	2.482	20	3.0
C6 [#]	24.5	49.1	58.71	2.534	20	4.0
C7 [#]	25.2	51.3	62.92	2.459	20	5.0
C15 [#]	25.1	53.2	64.34	2.444	20	0

D Diameter, H height, M mass, ρ density, σ_3 confining pressure, P_g gas seepage pressure

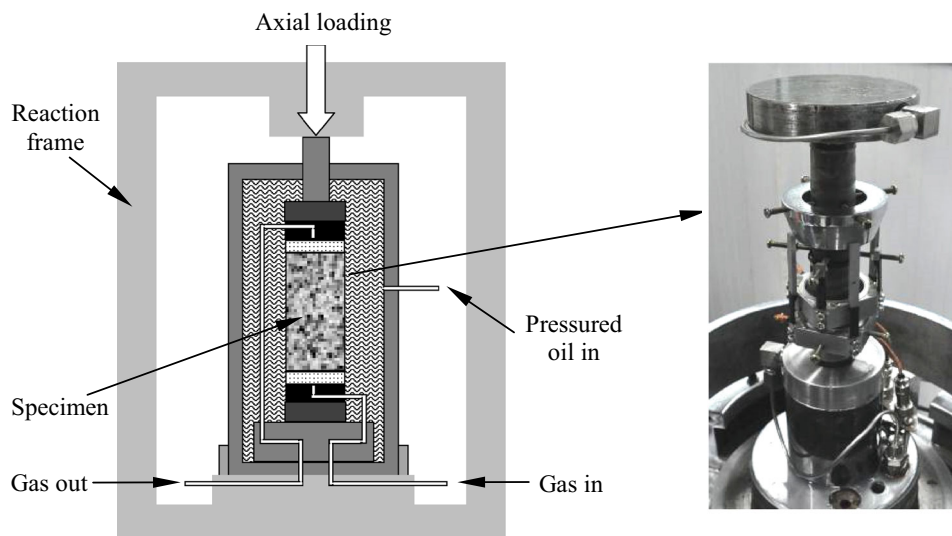


Fig. 2 Experimental configuration and specimen assembly

2.2 Loading procedure

The conventional triaxial compression and gas seepage tests were all carried out in a TAW-1000 triaxial rock mechanics experimental system with the maximum loading capacity of 1000 kN. This servo-controlled testing system can test specimens in load or displacement control mode while the data are recorded and analyzed in real-time by computer. In order to record the axial deformation, we use an axial dis-

placement transducer with a range of 4.0 mm, while the radial deformation was measured using a radial displacement transducer, for which the maximum displacement capacity was 2.0 mm. The detailed structures of the triaxial cell and the specimen installation are illustrated in Fig. 2. It should be pointed out that TAW-1000 triaxial rock mechanics experimental system is a stiff machine, which can be used to measure the strength and deformation parameters of rock materials even for the hard granite. The role of pressurized

oil shown in Fig. 2 is to apply the confining pressure on the tested specimen.

At the same time, in order to analyze the seepage evolution behavior of sandstone with different gas pressure in the process of deformation, the confining pressure is kept a constant, i.e. 20 MPa. The gas pressure is designed at four different values, i.e. 2, 3, 4, and 5 MPa. To form the seepage pressure difference, the pressure on one axial surface of the specimen is applied by nitrogen, and another axial surface of the specimen is connected with the atmosphere. Firstly, the conventional triaxial compression test at a confining pressure of 20 MPa is carried out on one sandstone specimen, which can be compared to the seepage experiment. Then, we carry out the seepage test with different gas pressure in the process of deformation.

The procedures of gas seepage experiment can be described as follows. Firstly, the confining pressure of 20 MPa is applied to the specimen at a rate of 0.5 MPa/s. Then, a gas pressure is applied to the specimens. Afterwards, keeping the confining pressure and gas pressure constant, the axial deviatoric stress was stepwise increased under displacement-controlled conditions with a rate of 0.04 mm/min until specimen failure. After each stress increment is applied, the volume flow through the specimen can be measured by using a soap bubble flowmeter. Thus, we can obtain the evolution curve of permeability of sandstone specimen during the entire loading.

For the type of rock materials whose permeability coefficient $k \geq 10^{-7} \mu\text{m}^2$, using the steady-state method to measure permeability is a better choice [23]. In this research, the permeability coefficient k of sandstone can be obtained by

$$k = \frac{2Qp_0\mu H}{(P_1^2 - P_2^2)A}, \quad (1)$$

where Q is the gas volume flow; p_0 is the atmospheric pressure; μ is the gas viscosity coefficient, which is usually a constant for the same temperature; H is the specimen height; A is the end surface area; P_1 and P_2 are the gas absolute pressures at inlet and outlet, respectively.

3 Analysis of experimental results

The axial deviatoric stress–strain curve of sandstone under conventional triaxial compression at a confining pressure of 20 MPa is presented in Fig. 3. In the figure, ε_1 , ε_3 and ε_v represent the axial strain, radial strain, and volumetric strain, respectively, and $(\sigma_1 - \sigma_3)$ is the deviatoric stress. From Fig. 3, it can be seen that the post-peak behavior of sandstone shows obvious brittleness. According to conventional triaxial experimental results of sandstone, detailed mechanical parameters can be described as follows: the peak deviatoric stress

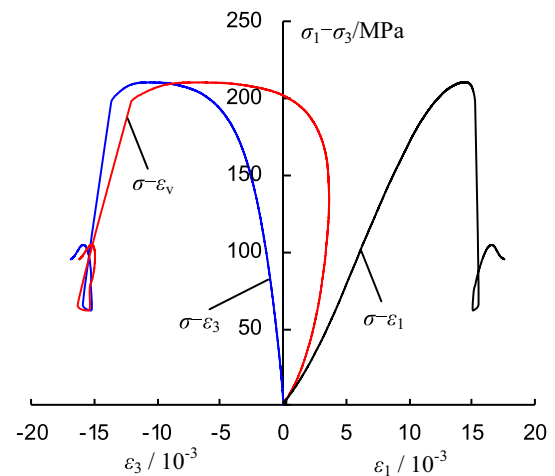


Fig. 3 Relation between deviatoric stress and axial strain, radial strain, and volumetric strain of sandstone under triaxial compression

is 210.47 MPa, the elastic modulus is 19.18 GPa, and the Poisson ratio is 0.245, while the peak axial strain, radial strain, and the volumetric strain corresponding to the peak strength are 14.303×10^{-3} , -10.215×10^{-3} and -6.128×10^{-3} , respectively.

The relationship between the permeability and the axial deviatoric stress–strain curve of sandstone under different gas seepage pressures is presented in Fig. 4. It should be noted that a series of small platforms in the stress–strain curves are induced by keeping the stress as a constant to measure the permeability of sandstone specimen. Furthermore, the platform is appreciable in comparison with the whole curve; therefore, strain increments can be ignored. From Fig. 4, it can be seen that the evolution of permeability can be divided into the following five phases: the phase of micro-defects closure (Region I), the phase of linear elastic deformation (Region II), the phase of nonlinear deformation (Region III), the phase of post-peak stress softening (Region IV), and the phase of residual strength (Region V). The detailed descriptions on permeability evolution process can be described as follows.

In Region I, due to the closure of the pre-existing micro-pores, micro-cracks, and other micro-defects, the gas seepage channels become smaller and fewer. The permeability decreases with the increase of strain, for example, the permeability of C7[#] specimen decreases from 1.770×10^{-3} to $1.150 \times 10^{-3} \mu\text{m}^2$.

In Region II, with the increase of deformation, the specimens continue to be compressed, so the gas seepage channels become smaller gradually. When the deviatoric stress increases to a certain extent, micro-cracks begin to form. The permeability coefficient firstly decreases and then increases as the strain increases. For example, the permeability of C7[#] specimen decreases from 1.150×10^{-3} to $1.061 \times 10^{-3} \mu\text{m}^2$, then increases from 1.061×10^{-3} to $1.611 \times 10^{-3} \mu\text{m}^2$.

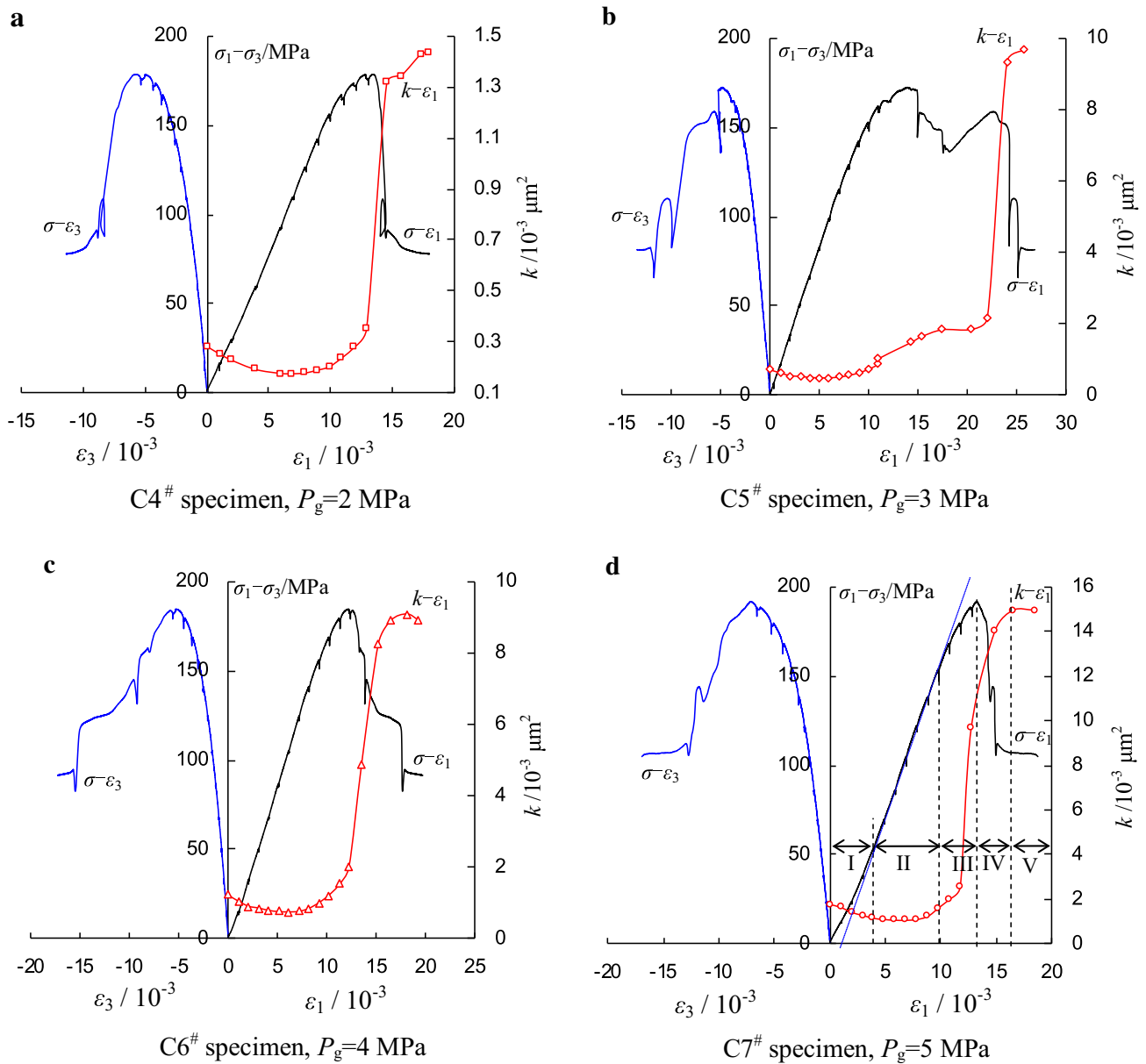


Fig. 4 Relation between permeability and axial strain of sandstone under different gas seepage pressures

In Region III, with further increase of deformation, the axial deviatoric stress continues to increase. The micro-cracks start to propagate and coalesce, resulting in bigger and more seepage channels. Obviously, the permeability rapidly increases. Take C7[#] specimen as an example; its permeability varies from 1.611×10^{-3} to $12.113 \times 10^{-3} \mu\text{m}^2$. It should be noted that the permeability does not reach the maximum value at peak strength, since the seepage channels continue to increase.

In Region IV, some macro-cracks are often induced by the coalescence of some micro-cracks, and at the same time, new micro-cracks are formed. These macro- and micro-cracks will result in continuous increase of the permeability, for

instance, the permeability of C7[#] specimen increases from 12.113×10^{-3} to $14.940 \times 10^{-3} \mu\text{m}^2$.

In Region V, when the stress reduces to the residual strength, macro-failure mode is formed on the whole. In other words, the seepage channels keep stable. Therefore, the permeability of rock basically keeps as a constant, e.g. the permeability of C7[#] specimen is about $14.940 \times 10^{-3} \mu\text{m}^2$.

It should be noted that the permeability at peak strength is hard to be measured. But in Fig. 4, we catch the permeability whose stress is almost closed to the peak strength. In addition, we also record the permeability at the stage of residual strength. In short, Fig. 4 clearly shows the permeability evolution law during the com-

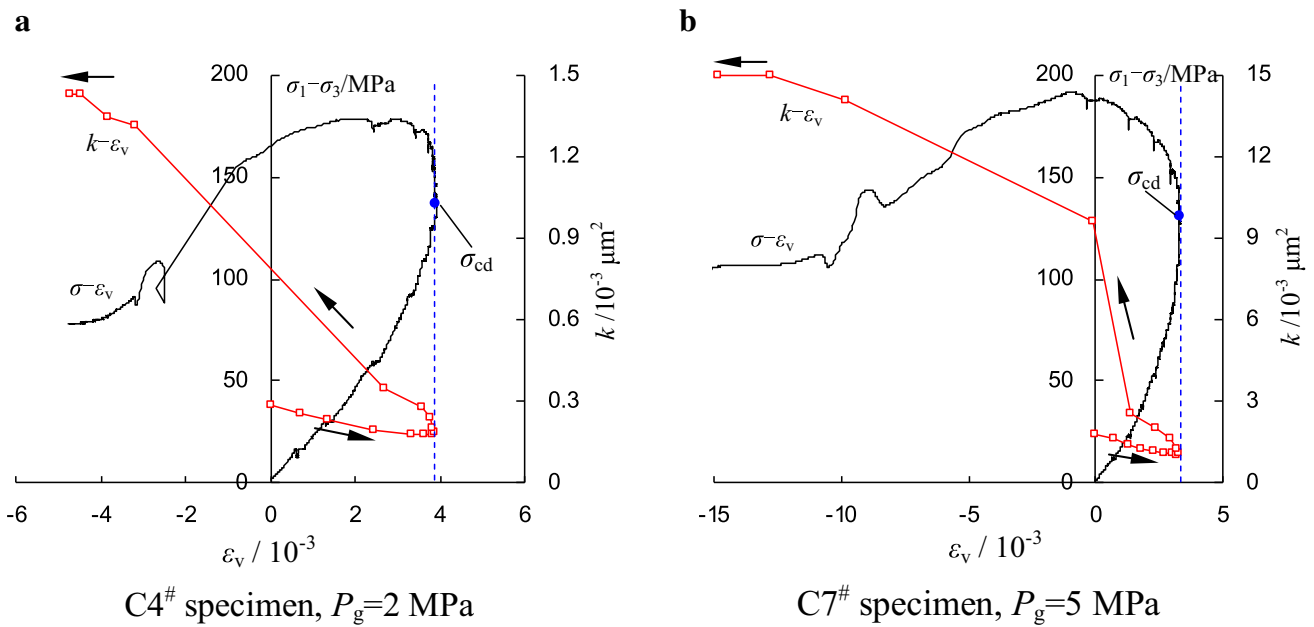


Fig. 5 Relation between permeability and volumetric strain of sandstone under different gas seepage pressures

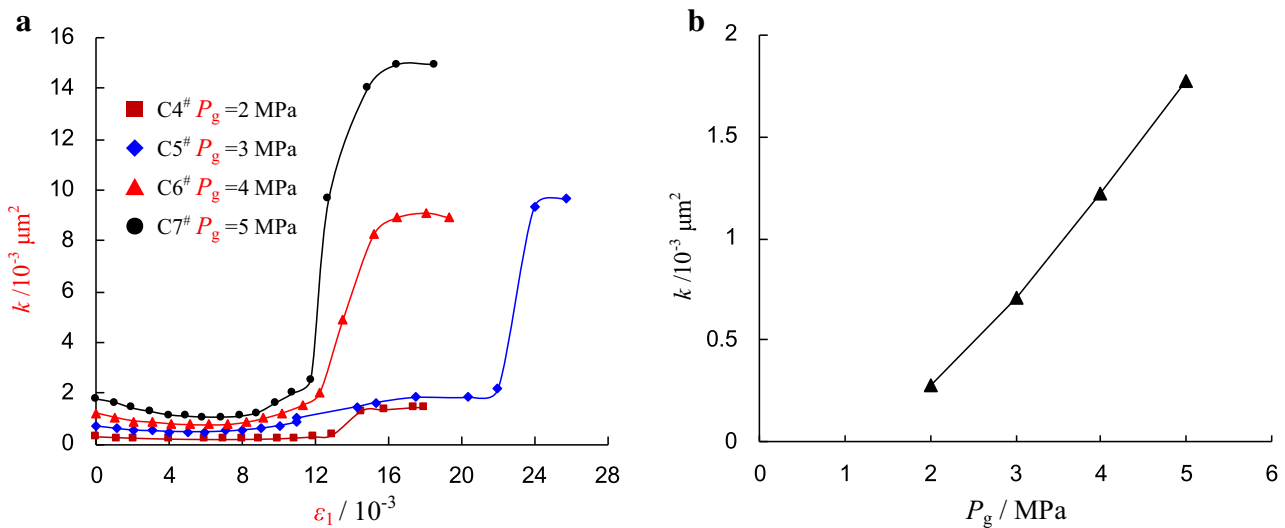


Fig. 6 Relation between permeability evolution curves and gas seepage pressures

plete sandstone failure process under triaxial compression.

The critical damage threshold [24] is a characterized stress during the rock failure, which can be determined from the axial deviatoric stress–volumetric strain curve, i.e. the corresponding stress where the volumetric strain switches from compaction to dilation. Figure 5 shows the relationship between permeability and volumetric strain of sandstone under different gas seepage pressures. As shown in Fig. 5, it is clear that the permeability evolution is closely correlated with the volumetric strain. At the stage of volumetric deformation compaction, permeability shows a decreasing

trend due to the closure of original micro-defects. But, at the stage of volumetric dilation, the propagation and coalescence of micro-cracks, and formation of macro-cracks all lead to an obvious increase of permeability. However, at the stage of residual strength, the permeability is unaffected by the deformation.

In order to investigate the effect of gas seepage pressure on the permeability evolution, the relationship between the permeability evolution curves and the gas seepage pressures is shown in Fig. 6a, while the relationship between the initial permeability and the gas seepage pressures is presented in Fig. 6b. It can be seen that the change trend

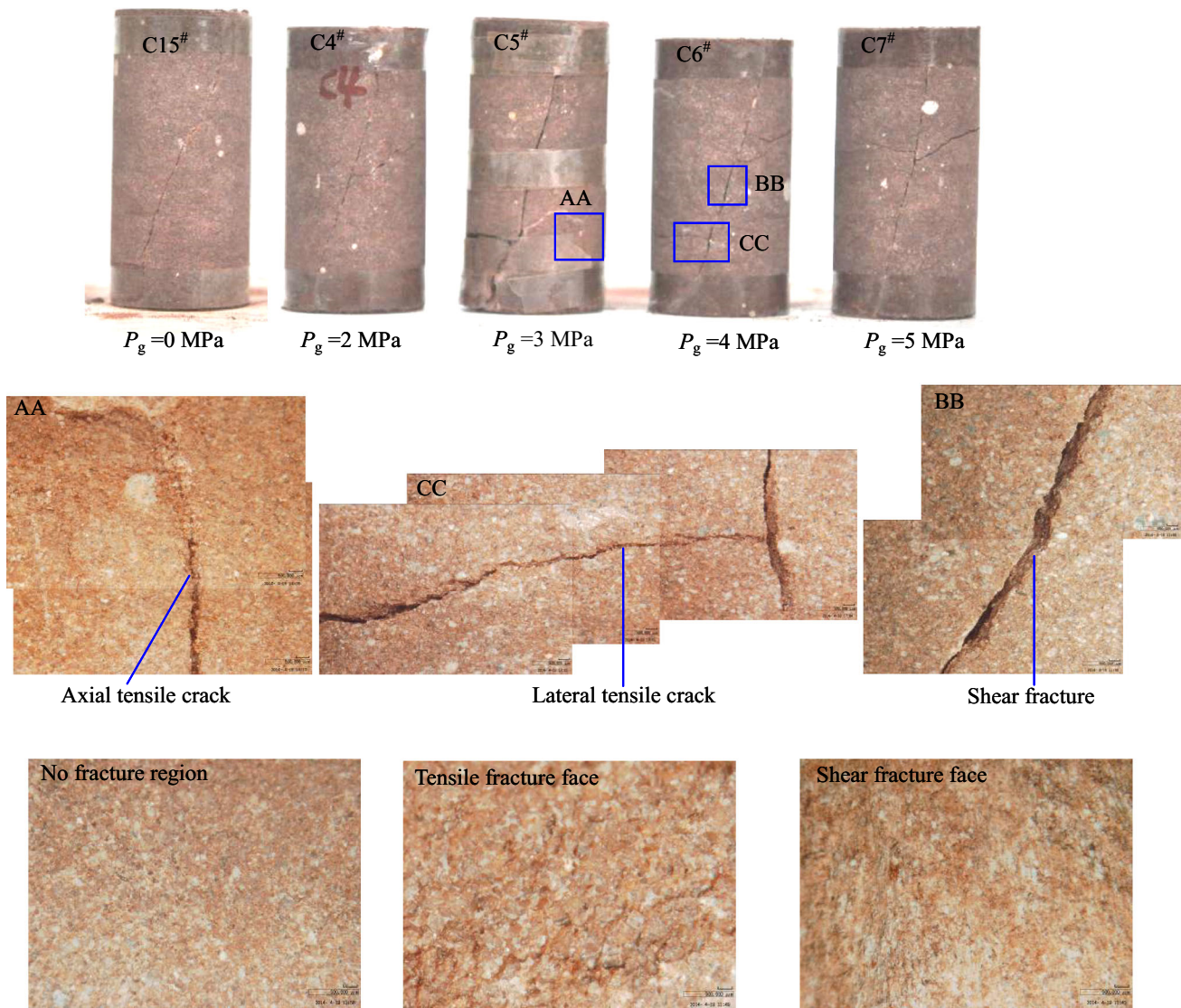


Fig. 7 Mixed tension and shear fracture mode of sandstone under different gas seepage pressures

of permeability–strain curves under different gas seepage pressures is basically similar, i.e. firstly, it decreases then increases, and finally tends to be stable. From Fig. 6, we can see that gas seepage pressure has an obvious effect on the permeability evolution characteristics, i.e. permeability increases with increasing gas seepage pressures. The variation trend can be explained from the effective confining pressure. When the confining pressure is kept constant, the increase of gas seepage pressure is equivalent to the reduction of effective confining pressure. Thus, the effective stress applying to the specimen actually becomes smaller, resulting in an increase of permeability.

The failure modes of sandstone under conventional triaxial compression and gas seepage tests are shown in Fig. 7. The failure behavior under conventional triaxial compression is different from that under gas seepage action. Under

conventional triaxial compression, the main shear plane is throughout the C15# specimen. Compared with the conventional triaxial compression, the failure modes under gas seepage tests are found to be more complicated. It can be seen that the sandstone specimens have multiple axial and lateral tensile cracks, besides the main shear fracture under gas seepage tests. From the microscopic observation images, we can see that the paths of crack coalescence are not smooth, which is the result of heterogeneity in sandstone material. The tensile fracture surface is found to be very rough due to brittle failure along the direction of the tensile crack plane. However, some powdery residues observed on the shear fracture surface indicate grain breakage. In addition, the shear fracture surface is found to be very flat, which may be the result of frictional sliding along the direction of the shear fracture plane.

4 Conclusions

In this paper, a series of experiments were carried out for sandstone specimens under conventional triaxial compression and gas seepage tests. Based on our test data, the following conclusions can be drawn. Coupled with the permeability–axial strain curve and deviatoric stress–axial strain curve, five stages of permeability evolution can be identified as follows: the phase of micro-defects closure, the phase of linear elastic deformation, the phase of non-linear deformation, the phase of post-peak stress softening, and the phase of residual strength. The seepage evolution characteristic is also closely correlated with the volumetric deformation according to the relationship between permeability and volumetric strain. The volumetric strain value corresponding to the critical damage threshold divides permeability evolution curve into three stages, i.e. the stages of decreasing, increasing and stabilization. It is found that the gas seepage pressure has a great effect on the permeability evolution, i.e. permeability increases with increasing gas seepage pressures. The failure mode of sandstone varies from single shear fracture under conventional triaxial compression to mixed tension and shear fracture under gas seepage tests.

Acknowledgments This project was supported by the National Natural Science Foundation of China (Grant 41272344), the National Basic Research Program (973) of China (Grant 2014CB046905), the Natural Science Foundation of Jiangsu Province of China (Grant BK2012568), the Team Project Funded by 2014 Jiangsu Innovation and Entrepreneurship Program, and the Fundamental Research Funds for the Central Universities (China University of Mining and Technology) (Grants 2014YC10 and 2014XT03). Outstanding Innovation Team Project in China University of Mining and Technology (Grant 2014QN002). The authors would like to express their sincere gratitude to the editor and two anonymous reviewers for their valuable comments, which have greatly improved this paper.

References

- Schulze, O., Popp, T., Kern, H.: Development of damage and permeability in deforming rock salt. *Eng. Geol.* **61**, 163–180 (2001)
- Wang, J.A., Park, H.D.: Fluid permeability of sedimentary rocks in a complete stress–strain process. *Eng. Geol.* **63**, 291–300 (2002)
- Jiang, Q.H., Deng, S.S., Zhou, C.B., et al.: Modeling unconfined seepage flow using three-dimensional numerical manifold method. *J. Hydrodyn.* **22**, 554–561 (2010)
- Zhang, R., Jiang, Z., Sun, Q., et al.: The relationship between the deformation mechanism and permeability on brittle rock. *Nat. Hazards* **66**, 1179–1187 (2013)
- Ma, D., Miao, X.X., Chen, Z.Q., et al.: Experimental investigation of seepage properties of fractured rocks under different confining pressures. *Rock Mech. Rock Eng.* **46**, 1135–1144 (2013)
- Wang, H.L., Xu, W.Y., Shao, J.F.: Experimental researches on hydro-mechanical properties of altered rock under confining pressures. *Rock Mech. Rock Eng.* **47**, 485–493 (2014)
- Tan, X., Konietzky, H., Frühwirth, T.: Laboratory observation and numerical simulation of permeability evolution during progressive failure of brittle rocks. *Int. J. Rock Mech. Min. Sci.* **68**, 167–176 (2014)
- Alam, A.K.M., Niioka, M., Fujii, Y., et al.: Effects of confining pressure on the permeability of three rock types under compression. *Int. J. Rock Mech. Min. Sci.* **65**, 49–61 (2014)
- Li, S.P., Wu, D.X., Xie, W.H., et al.: Effect of confining pressure, pore pressure and specimen dimension on permeability of Yinzhuang sandstone. *Int. J. Rock Mech. Min. Sci.* **34**, 175–186 (1997)
- Souley, M., Homand, F., Pepa, S., et al.: Damage-induced permeability changes in granite: a case example at the URL in Canada. *Int. J. Rock Mech. Min. Sci.* **38**, 297–310 (2001)
- Heiland, J.: Laboratory testing of coupled hydro-mechanical processes during rock deformation. *Hydrol. J.* **11**, 122–141 (2003)
- Yang, T.H., Liu, J., Zhu, W.C., et al.: A coupled flow-stress-damage model for groundwater outbursts from an underlying aquifer into mining excavations. *Int. J. Rock Mech. Min. Sci.* **44**, 87–97 (2007)
- Qi, Q., Li, H., Wang, Y., et al.: Theory and test research on permeability of coal and rock body influenced by mining. *J. Coal Sci. Eng.* **15**, 143–147 (2009). (in Chinese)
- Zhou, J.J., Shao, J.F., Xu, W.Y.: Coupled modeling of damage growth and permeability variation in brittle rocks. *Mech. Res. Commun.* **33**, 450–459 (2006)
- Wang, H., Chu, W., He, M.: Anisotropic permeability evolution model of rock in the process of deformation and failure. *J. Hydrodyn.* **24**, 25–31 (2012)
- Pereira, J.M., Arson, C.: Retention and permeability properties of damaged porous rocks. *Comput. Geotech.* **48**, 272–282 (2013)
- Huang, T., Rudnicki, J.W.: A mathematical model for seepage of deeply buried groundwater under higher pressure and temperature. *J. Hydrol.* **327**, 42–54 (2006)
- Chen, Y., Hu, R., Lu, W., et al.: Modeling coupled processes of non-steady seepage flow and non-linear deformation for a concrete-faced rockfill dam. *Comput. Struct.* **89**, 1333–1351 (2011)
- Levasseur, S., Collin, F., Charlier, R., et al.: A micro–macro approach of permeability evolution in rocks excavation damaged zones. *Comput. Geotech.* **49**, 245–252 (2013)
- Tang, C.A., Tham, L.G., Lee, P.K.K., et al.: Coupled analysis of flow, stress and damage (FSD) in rock failure. *Int. J. Rock Mech. Min. Sci.* **39**, 477–489 (2002)
- Jiang, T., Shao, J.F., Xu, W.Y., et al.: Experimental investigation and micromechanical analysis of damage and permeability variation in brittle rocks. *Int. J. Rock Mech. Min. Sci.* **47**, 703–713 (2010)
- Ou, S., Wang, L., Wang, P., et al.: Numerical analysis of seepage flow characteristic of collapse column under the influence of mining. *Int. J. Min. Sci. Technol.* **23**, 237–244 (2013)
- Davy, C.A., Skoczylas, F., Barnichon, J.D., et al.: Permeability of macro-cracked argillite under confinement: gas and water testing. *Phys. Chem. Earth* **32**, 667–680 (2007)
- Martin, C.D.: Seventeenth Canadian geotechnical colloquium: the effect of cohesion loss and stress path on brittle rock strength. *Can. Geotech. J.* **34**, 698–725 (1997)